From Model Magnetic Systems to Device Applications : μSR at TRIUMF and PSI

Sarah Dunsiger

Center for Emergent Materials
The Ohio State University

Magnetic Analogue of ice : a Model System

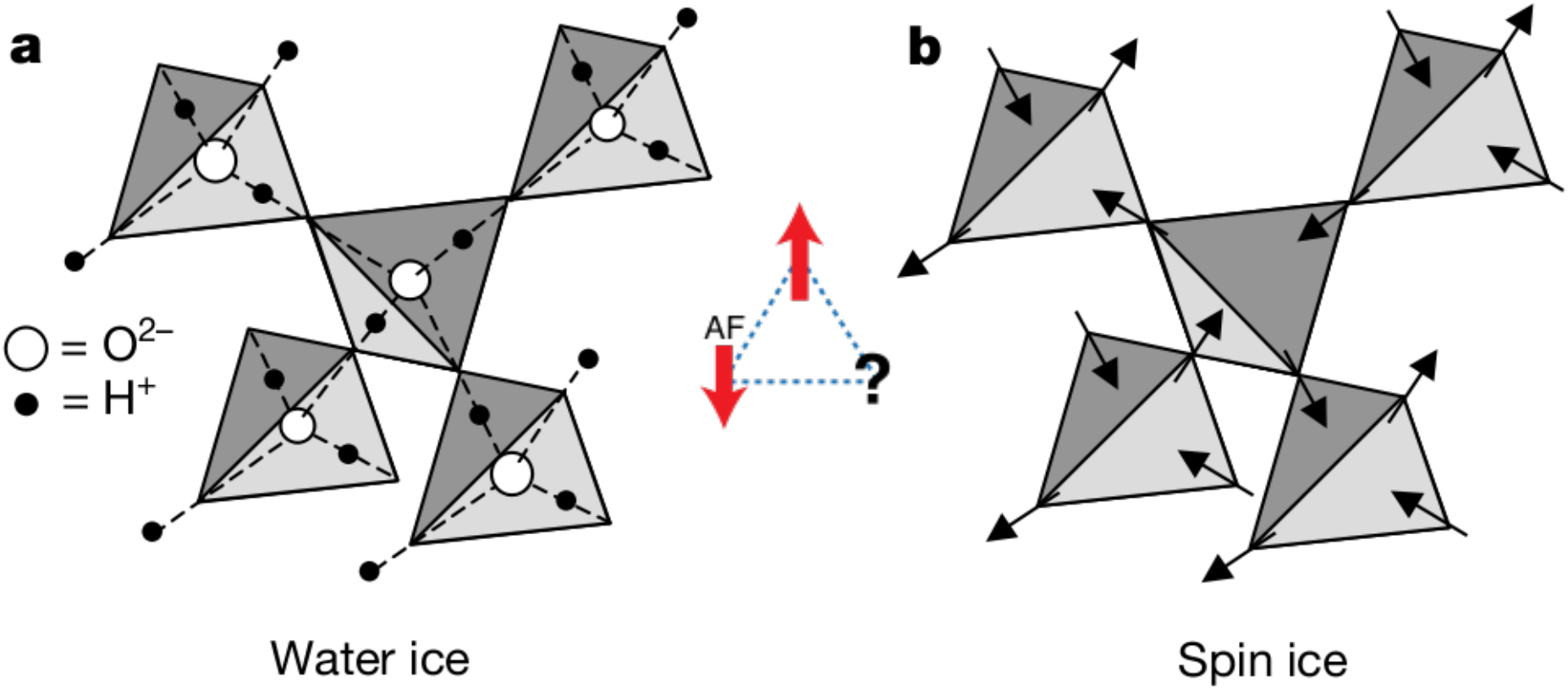

Strong [111] anisotropy

Phase diagram of Ising pyrochlore magnets with nearest neighbour exchange and long range dipolar interactions

$Tb_2Ti_2O_7$ (J=6 4f ^{8}) $Dy_2Ti_2O_7$ (J=15/2 4f ^{9}) $Ho_2Ti_2O_7$ (J=8 4f^{10})

$$H = -J\sum_{\langle ij\rangle} \mathbf{S}_i^{z_i}\cdot\mathbf{S}_j^{z_j} + Dr_{\mathrm{nn}}^3 \sum_{j>i} \frac{\mathbf{S}_i^{z_i}\cdot\mathbf{S}_j^{z_j}}{|\mathbf{r}_{ij}|^3} - \frac{3(\mathbf{S}_i^{z_i}\cdot\mathbf{r}_{ij})(\mathbf{S}_j^{z_j}\cdot\mathbf{r}_{ij})}{|\mathbf{r}_{ij}|^5}$$

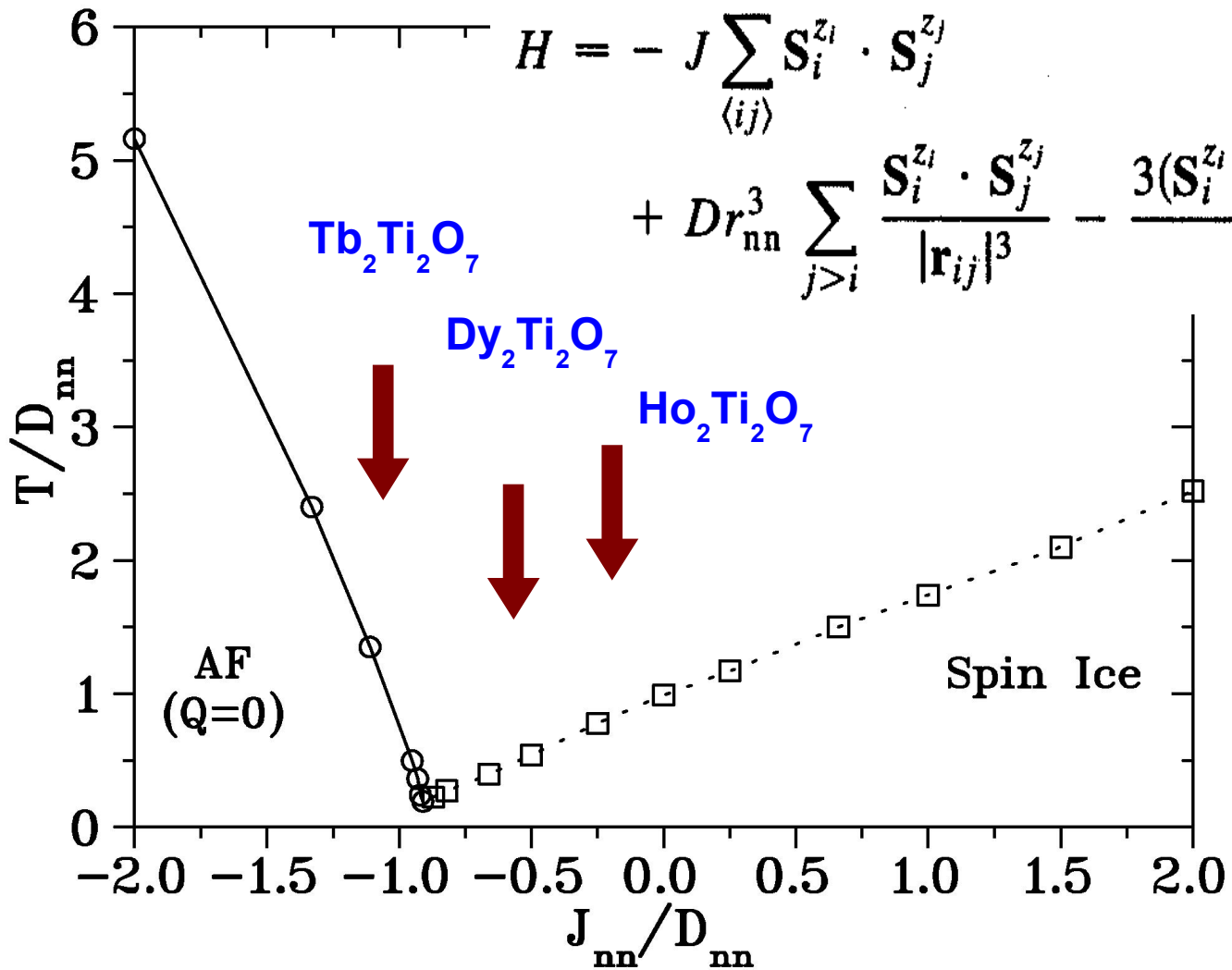

B. C. den Hertog and M. J. P. Gingras, PRL 84 3430 (2000)

Spectral Weight at non-zero Q: Diffuse Neutron Scattering in $Dy_2Ti_2O_7$ and $Ho_2Ti_2O_7$

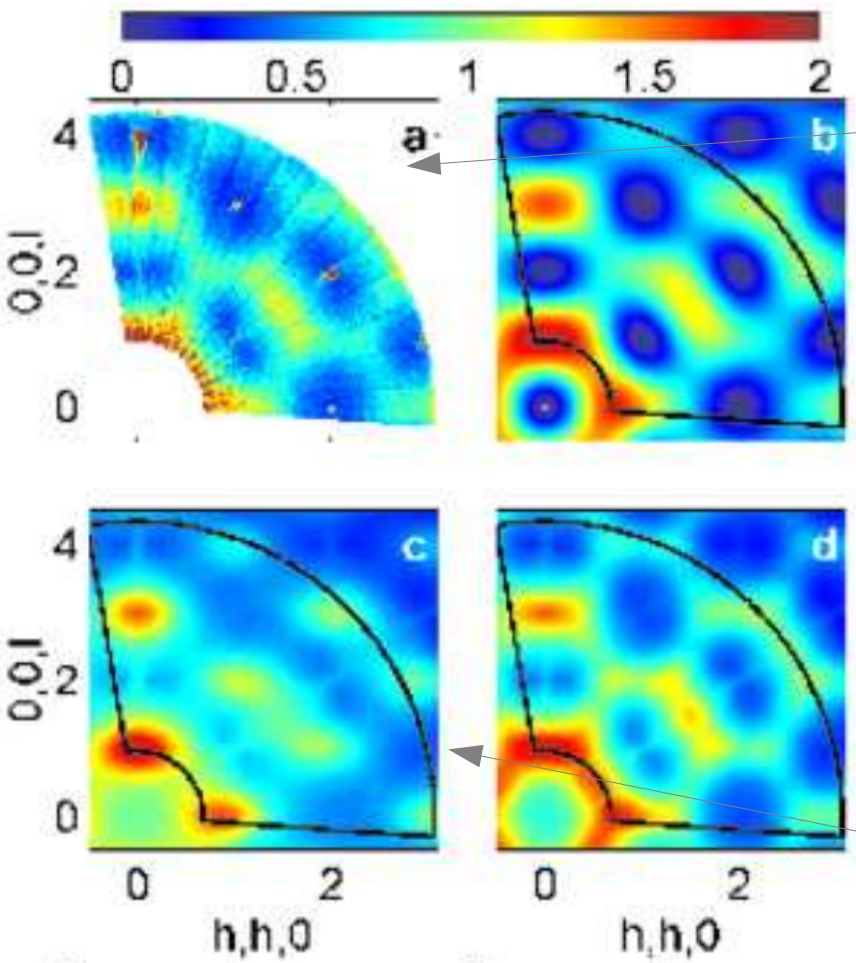

Experiment

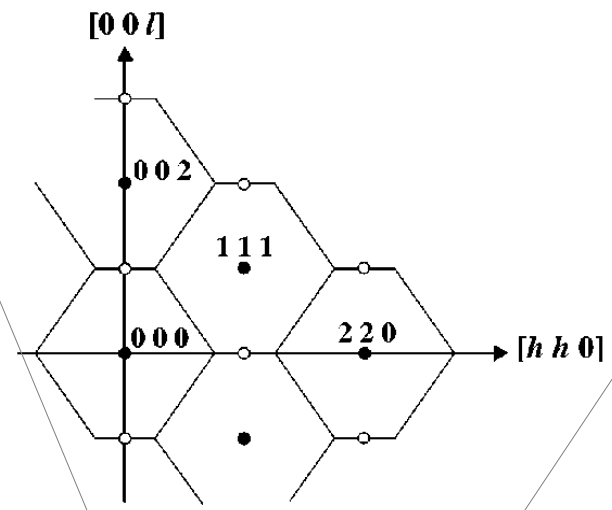

Theory

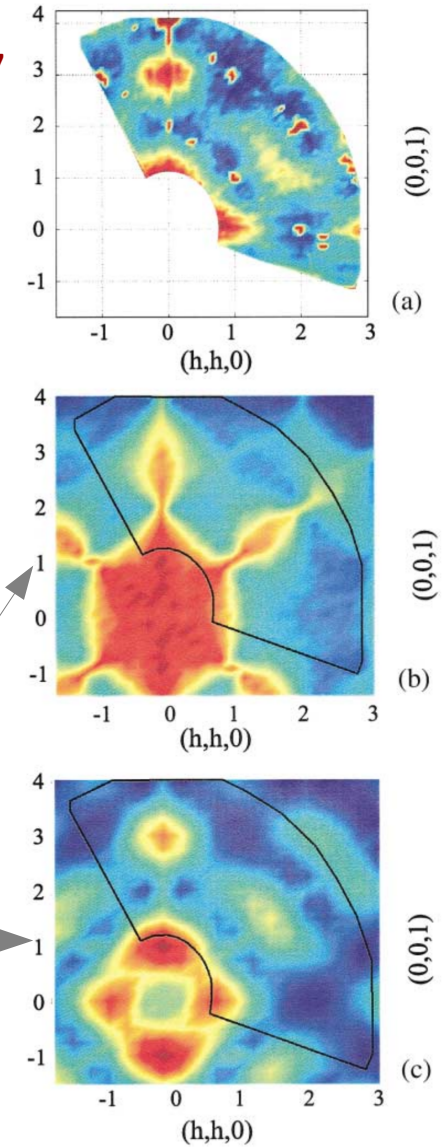

T. Fennell et al, PRB 70 134408 (2004)
T. Yavors'kii et al, PRL 101, 037204 (2008)

S. T. Bramwell et al, PRL 87 047205 (2001)

Magnetic Charges in Spin Ice

I. A. Ryzhkin, JETP 101, 481 (2005)
C. Castelnovo et al, Nature 451, 42 (2007)

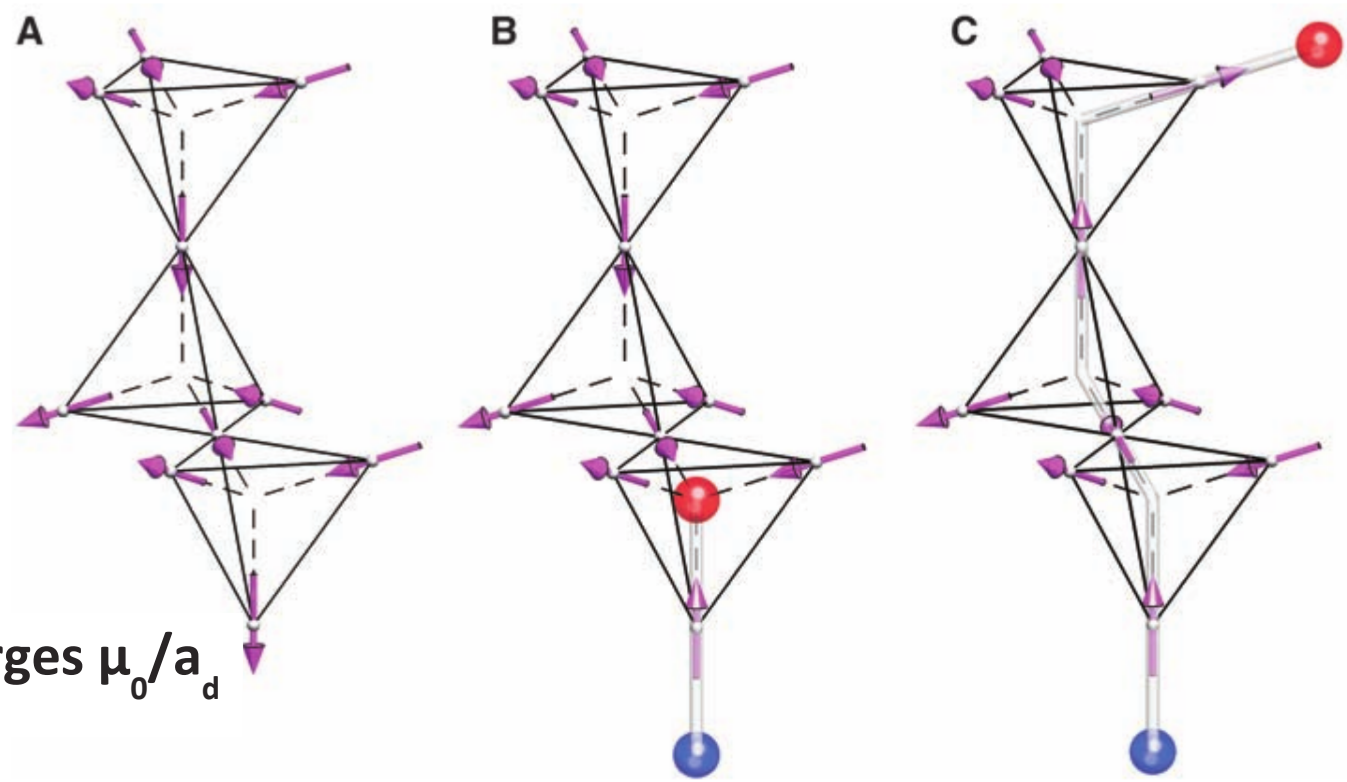

Magnetic charges μ_0/a_d

T. Fennell et al, Science 326, 415 (2009)
D. J. P. Morris et al, Science 326, 411 (2009)
S. T. Bramwell et al, Nature 461, 956 (2009)
L. D. C Jaubert, P. C. W. Holdsworth, Nature Phys 5, 258 (2009)

Thermally Activated Arrhenius Behaviour in Spin Ice

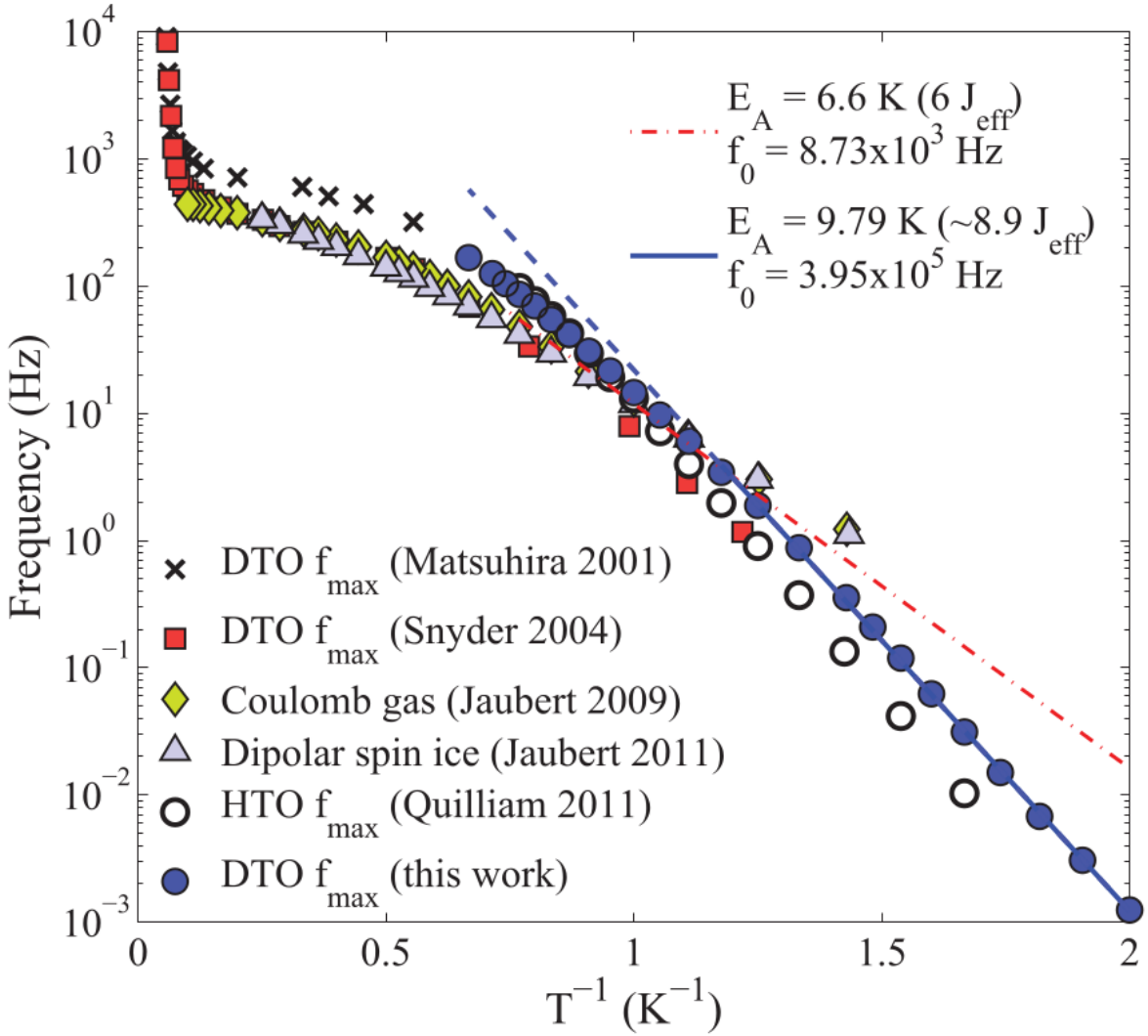

L R Yaraskavitch et al, Phys Rev B 85, 020410 (2012)

Experimental Probes on Complementary Timescales

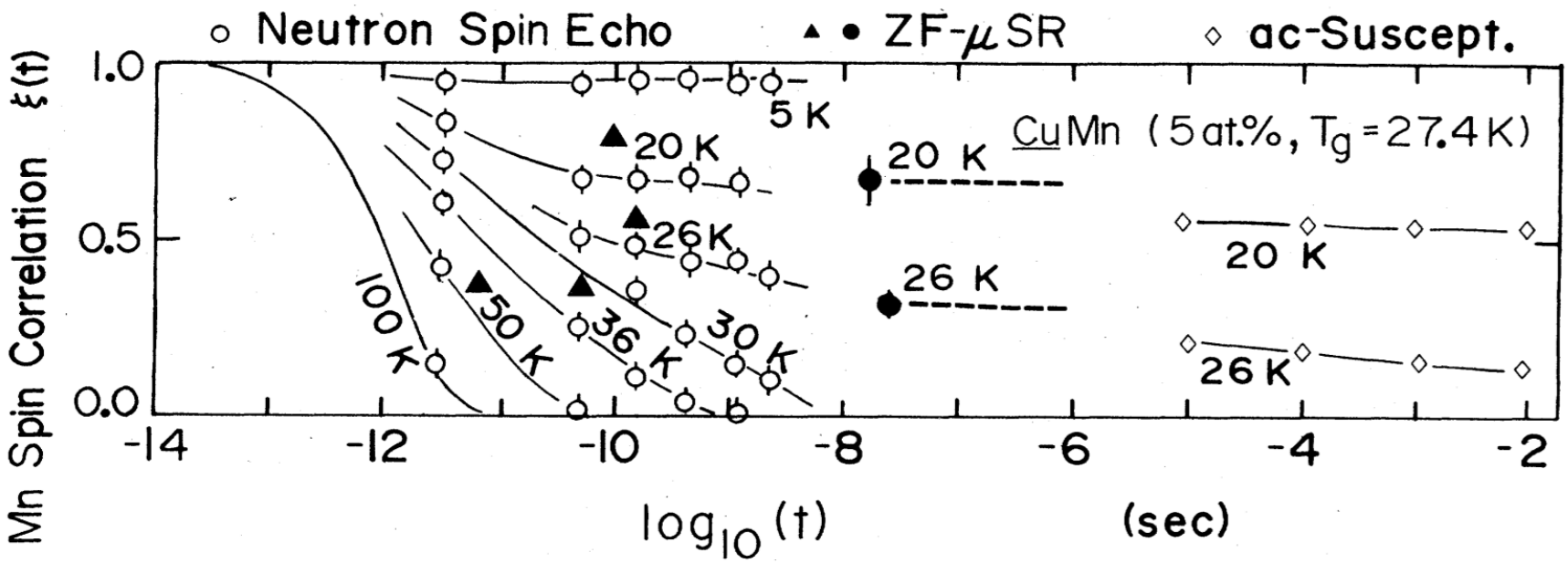

Local (Q resolved or Q averaged) versus Bulk techniques (Q=0)

Y J Uemura et al, Phys. Rev. B 31, 546 (1985)

Crossover from Exchange Narrowed to Broadened Regimes in $Dy_2Ti_2O_7$

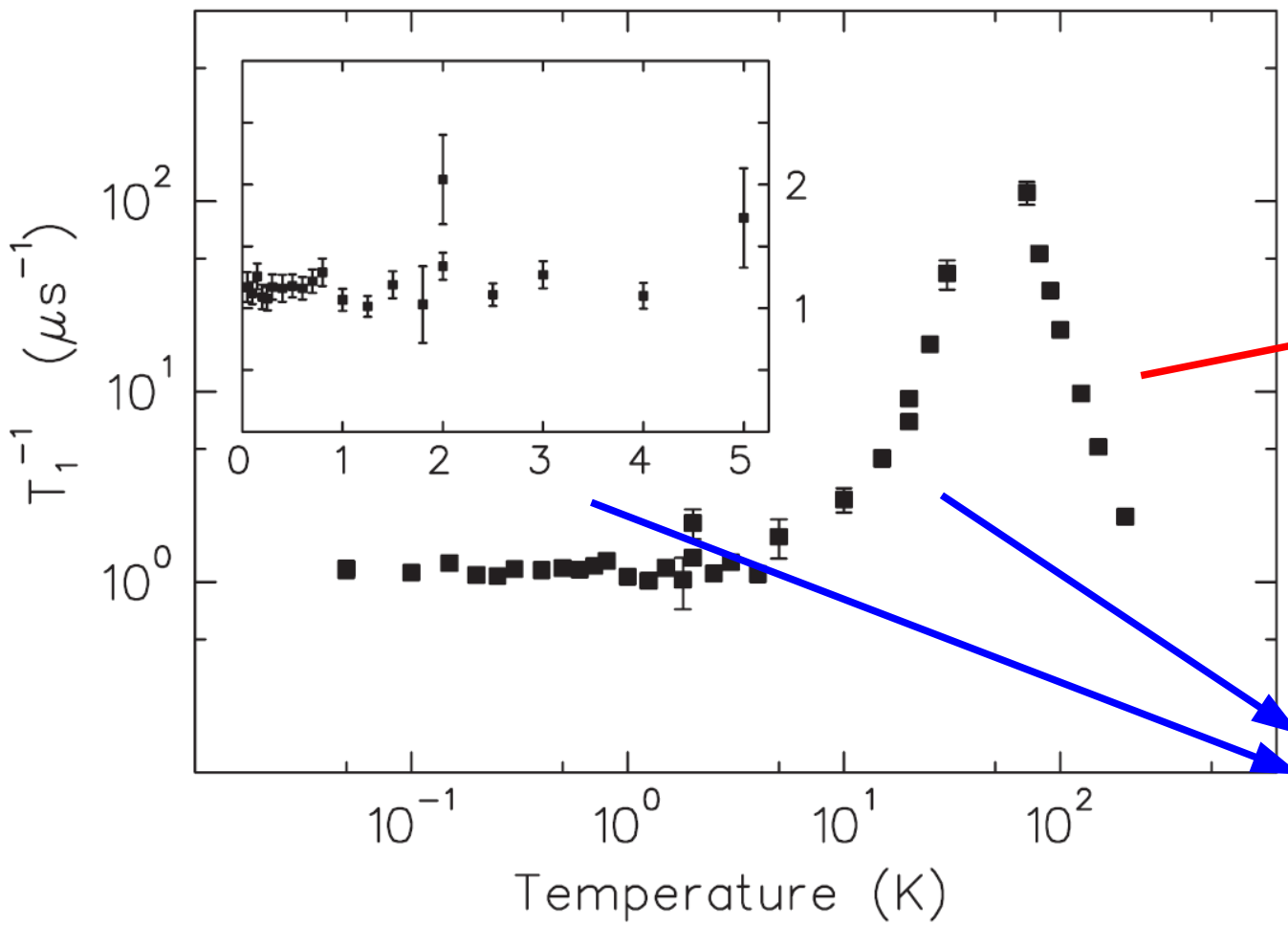

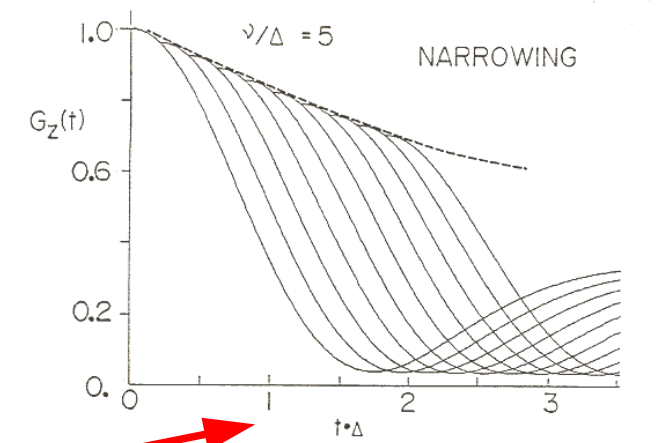

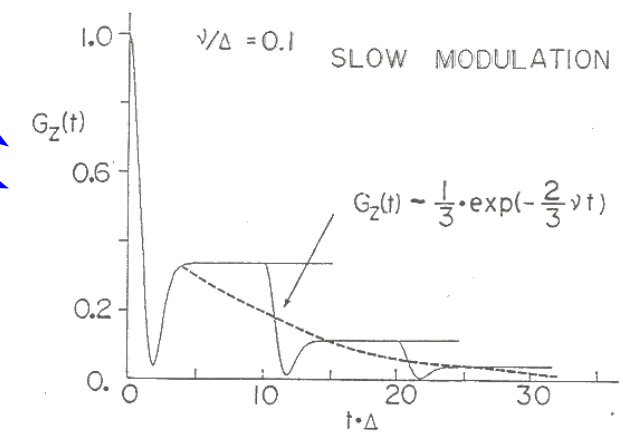

S R Dunsiger et al, PRL 107, 207207 (2011)

Quantum Spin Ice : Softening the Anisotropy

$Yb_2Ti_2O_7$ J=7/2 $4f^{13}$ g_{xy}/g_z =2.4

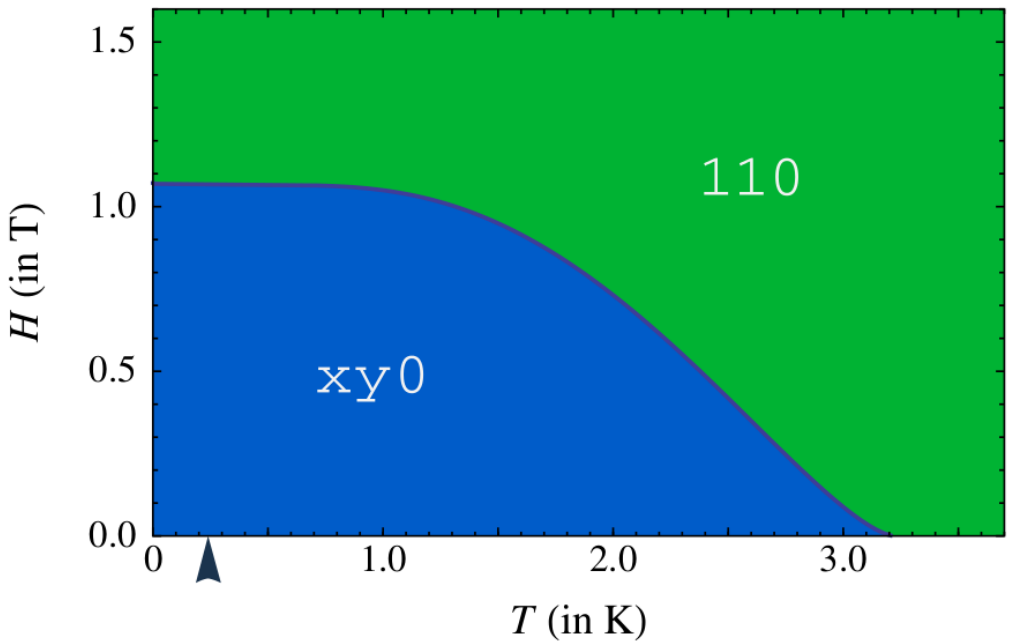

J_{zz}=0.17(4) meV; $J_{\pm}$=0.05(1);
$J_{\pm\pm}$=0.05(1); $J_{z\pm}$=0.14(1)

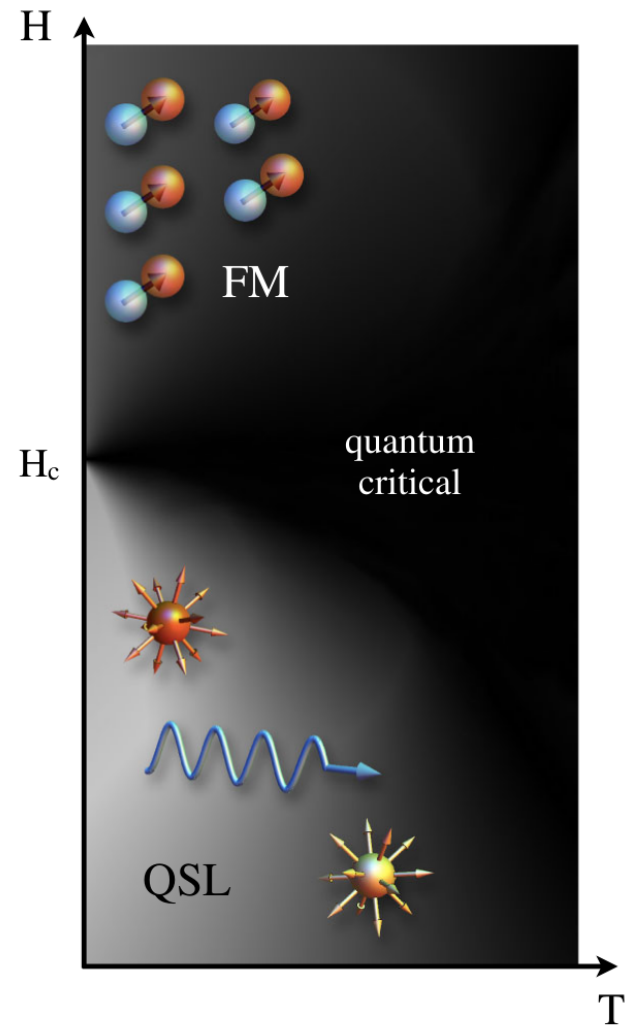

K A Ross et al, Phys Rev X 1, 021002 (2011)

Quantum Excitations in Quantum Spin Ice

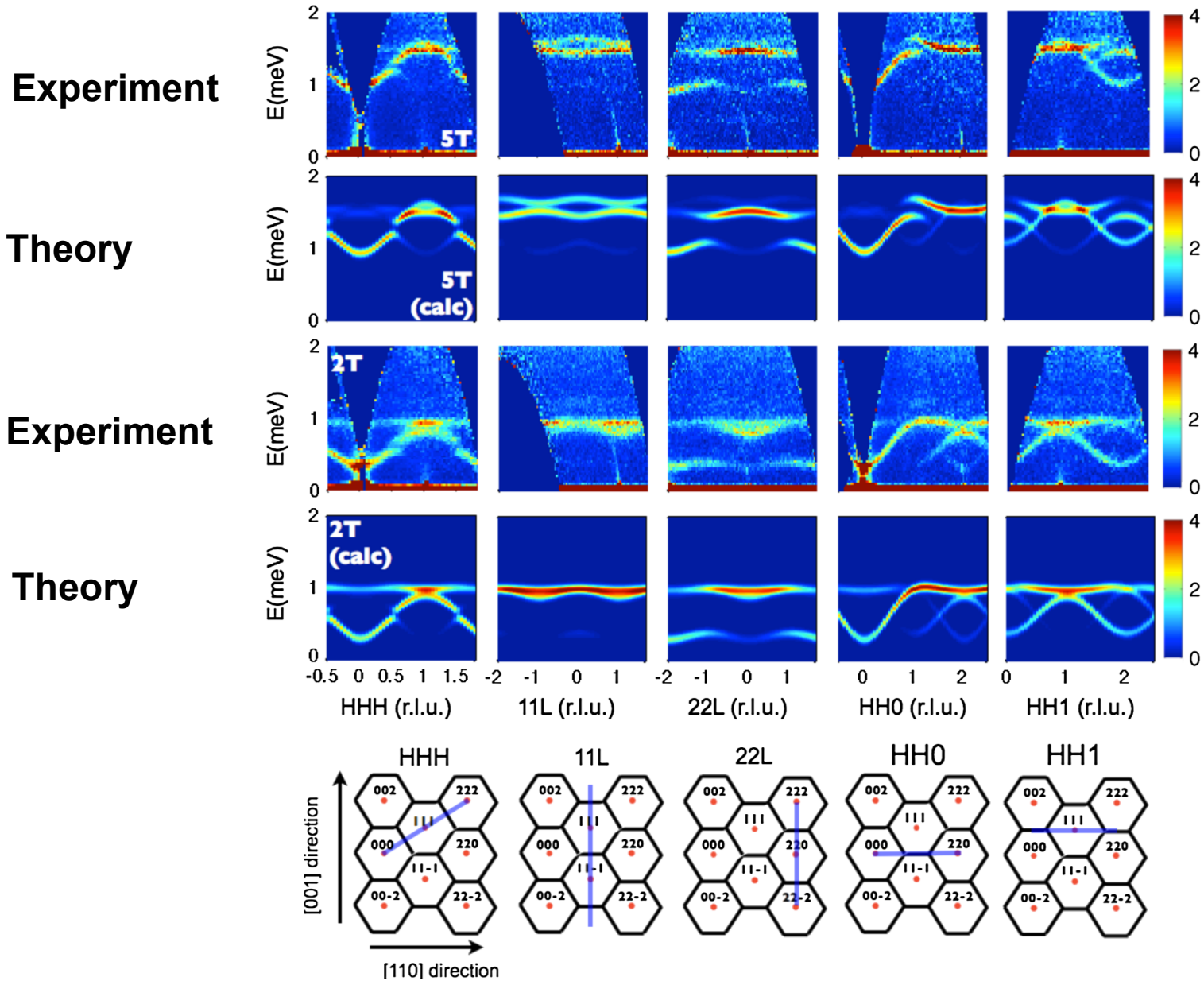

*K A Ross et al, Phys Rev X **1**, 021002 (2011)*

$Yb_2Ti_2O_7$: A Candidate Quantum Spin Liquid

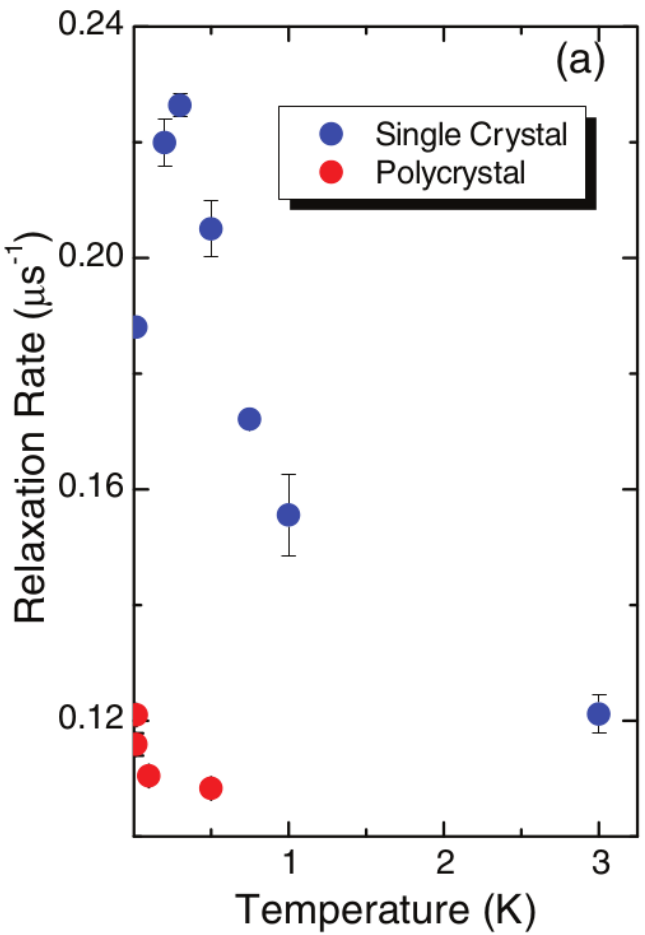

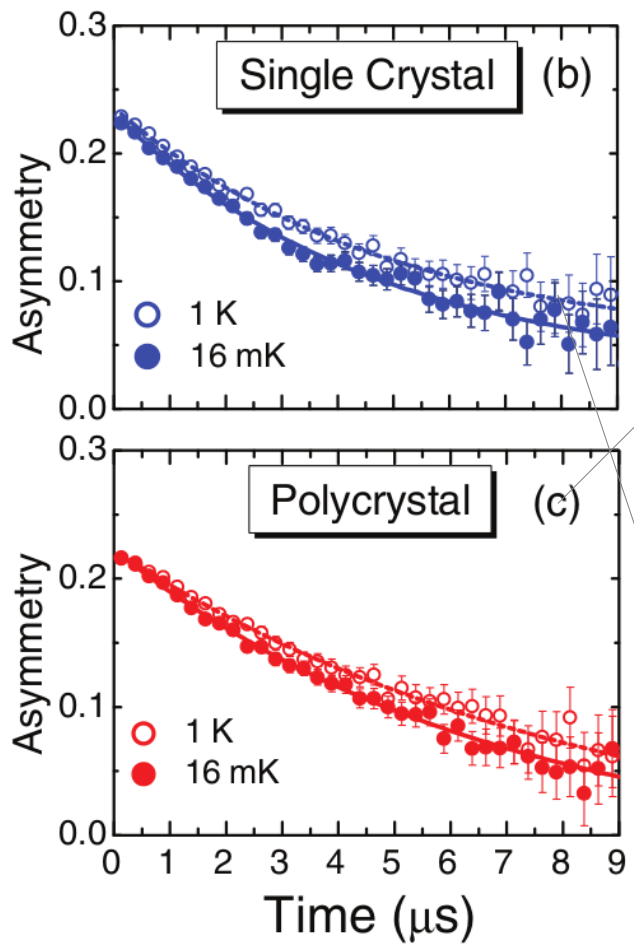

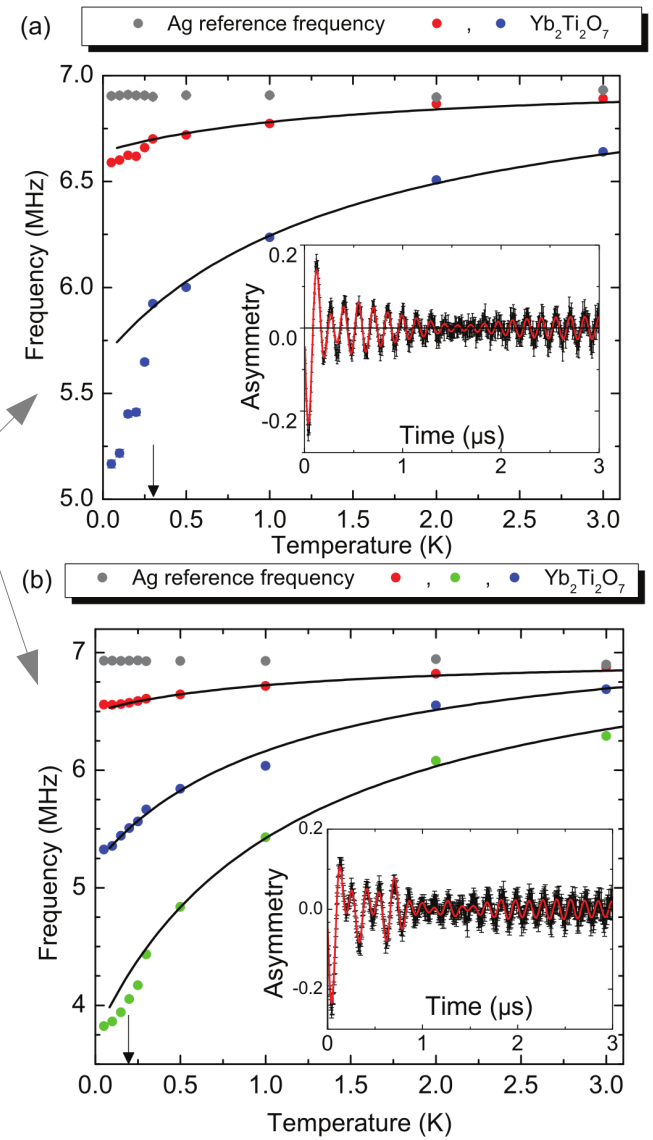

R M D'Ortenzio et al, Phys Rev B 88, 134428 (2013)

Ferromagnetic Transition and Metal-Insulator Transition in Doped $Ga_{1-x}Mn_xAs$

Sample	$x = 0.010$ as-grown	0.012 as-grown	0.030 as-grown	0.034 as-grown	0.034 annealed	0.070 as-grown	0.070 annealed
T_c from M	< 5 K	16 K	29 K	46 K	73 K	96 K	146 K
T_c from ρ	-	-	-	45 K	76 K	97 K	145 K

Ga : $[Ar]3d^{10}4s^2p^1$; Mn : $[Ar]3d^5 4s^2$; As : $[Ar]3d^{10}4s^2p^3$

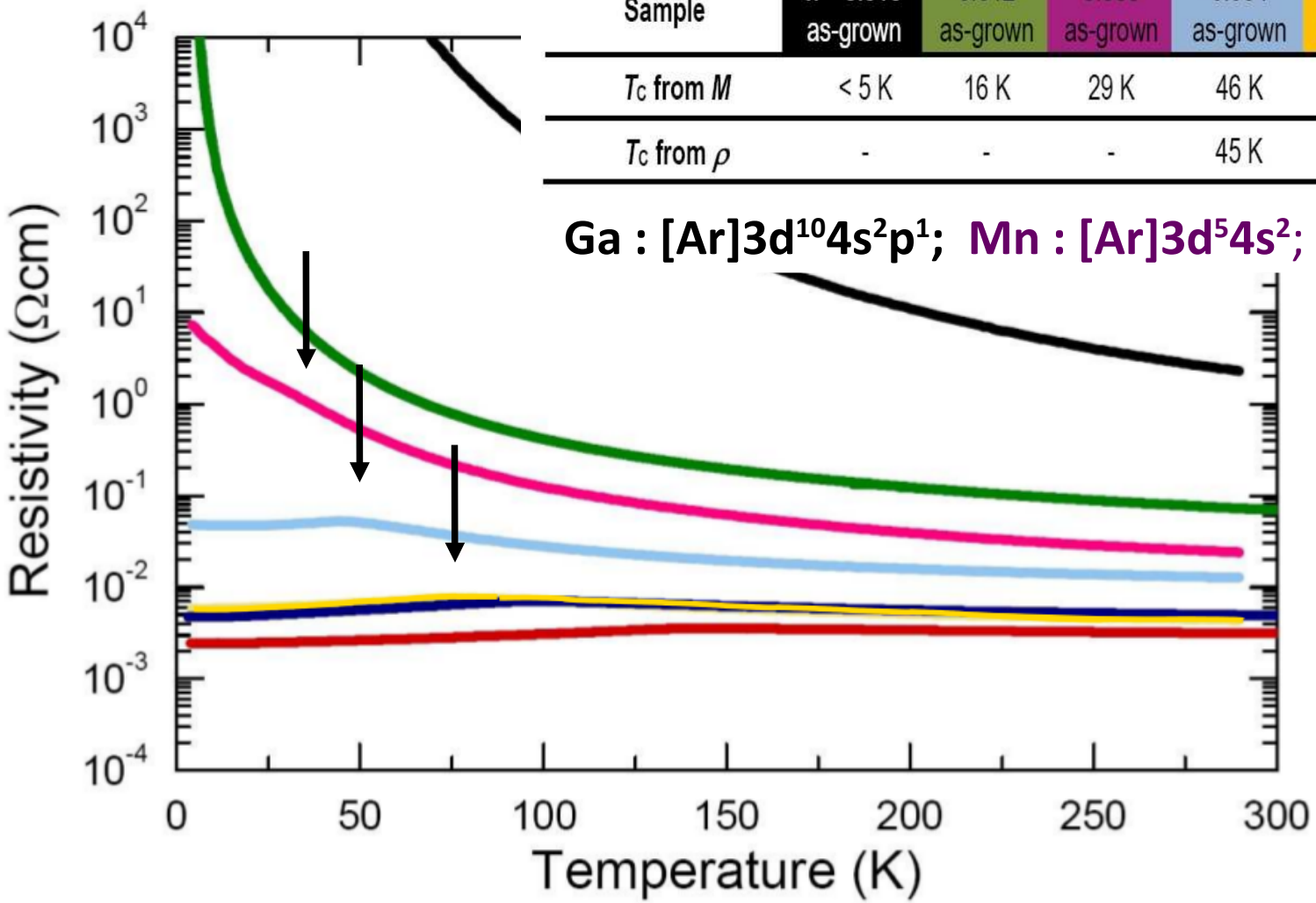

S. R. Dunsiger et al, Nature Mater 9, 299 (2010)

Tuning Hole Density in $Ga_{1-x}Mn_xAs$ (x=0.07) with Gate Voltage

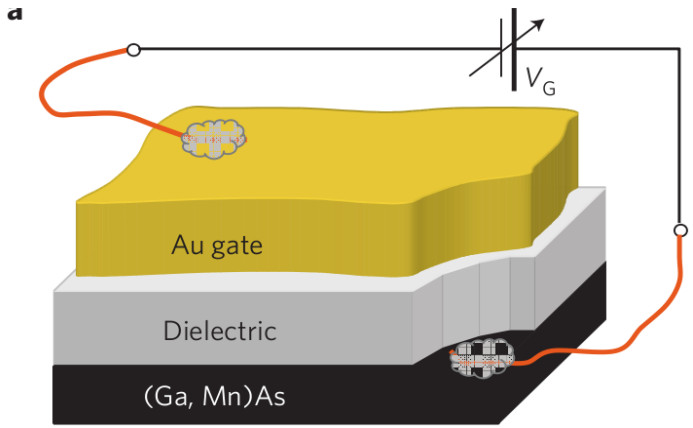

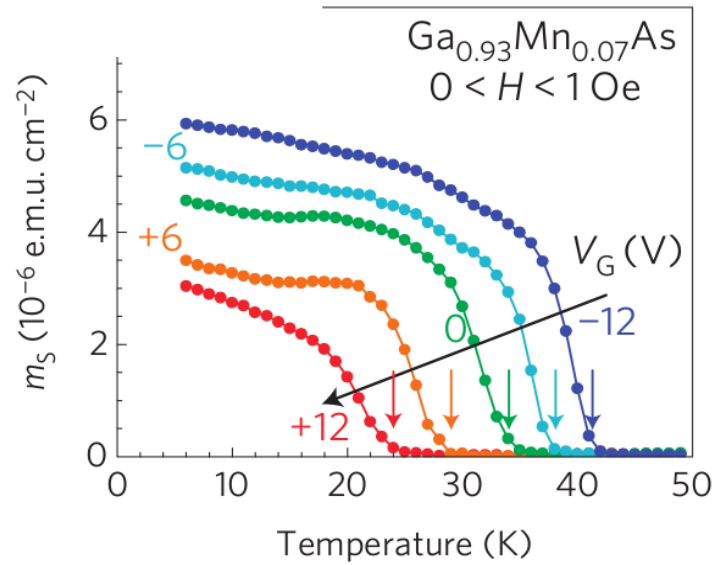

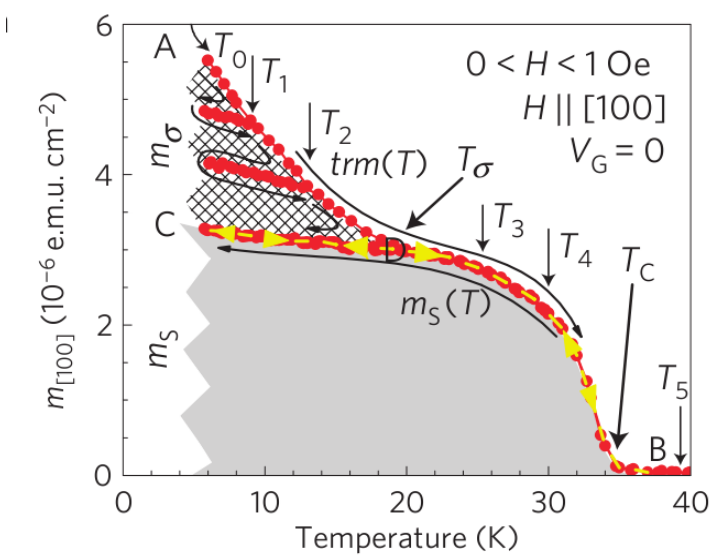

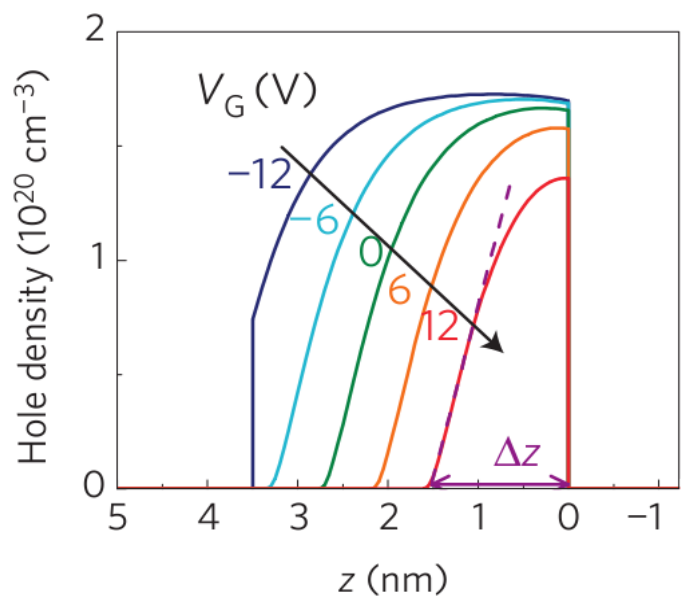

M. Sawicki et al, Nature Physics 6, 22 (2010)

Low energy μ^+ beam and set-up for LE-μSR (LEM)

- UHV system, 10^{-10} mbar
- some parts LN_2 cooled

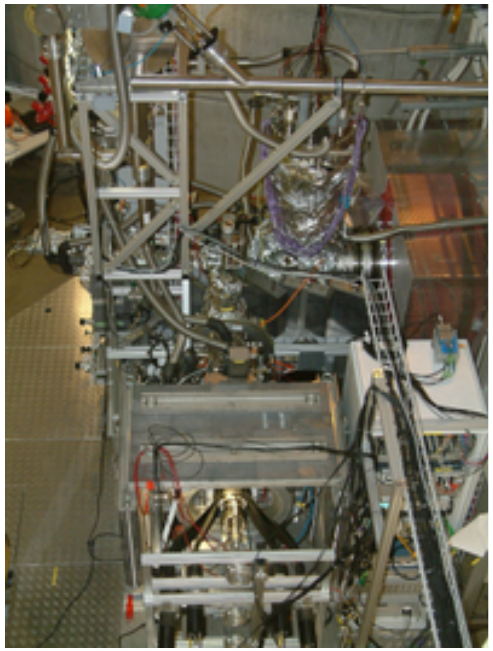

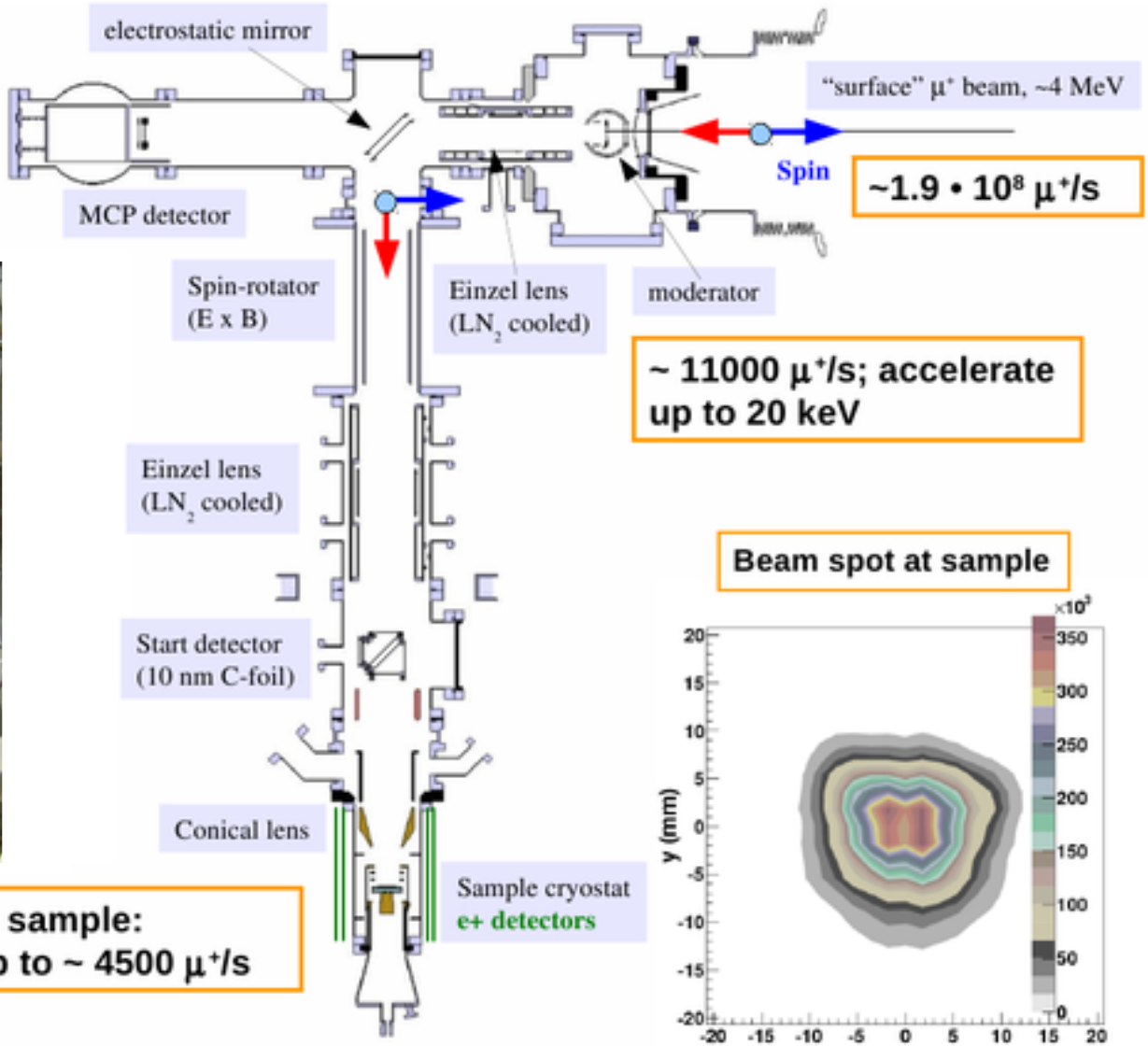

~1.9 • 10^8 μ^+/s

~ 11000 μ^+/s; accelerate up to 20 keV

at sample: up to ~ 4500 μ^+/s

Beam spot at sample

Low Energy μSR – Local Probe of Internal Magnetic Field Distribution on nanometre Lengthscales for Studies of Thin Films and Buried Interfaces

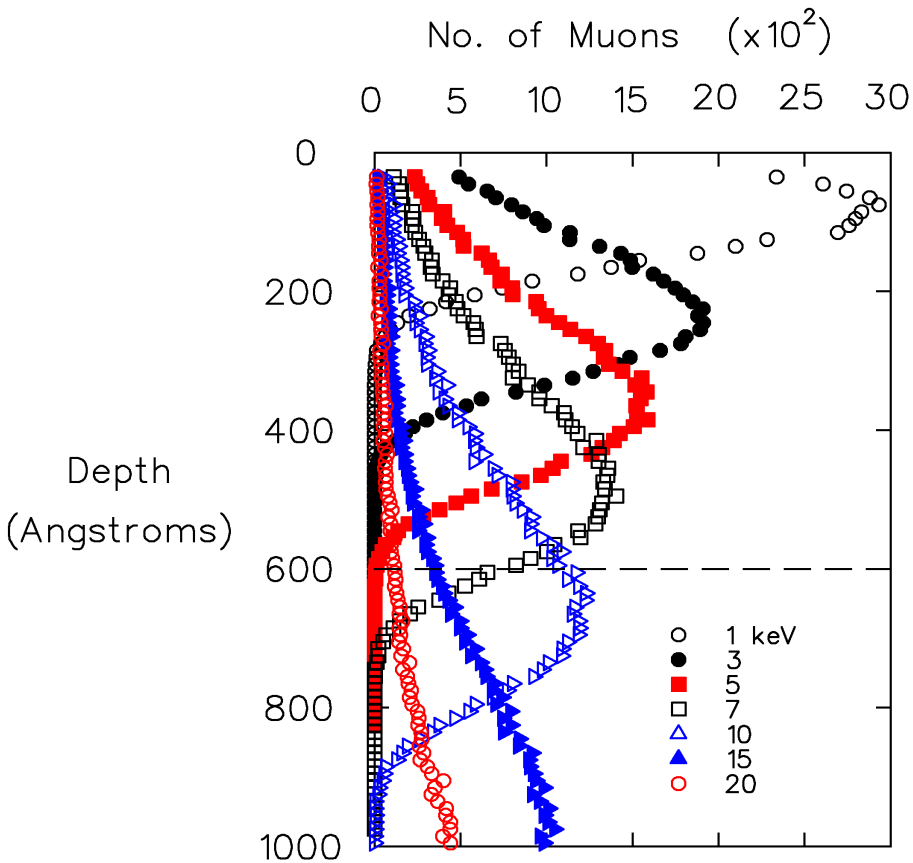

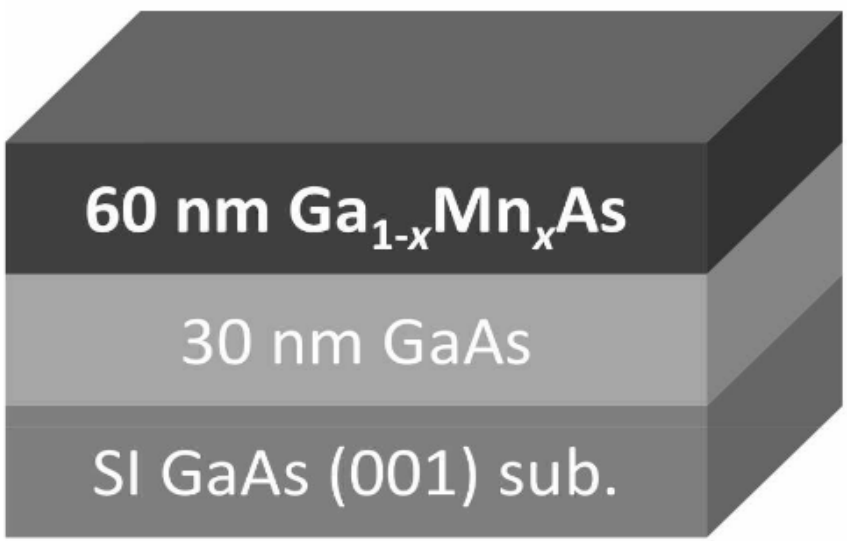

E. Morenzoni et al, J. Phys Condens Matt 16, S4583 (2004)

Systematic homogeneous spin freezing involving the entire volume fraction observed on both sides of the semiconducting-metal transition

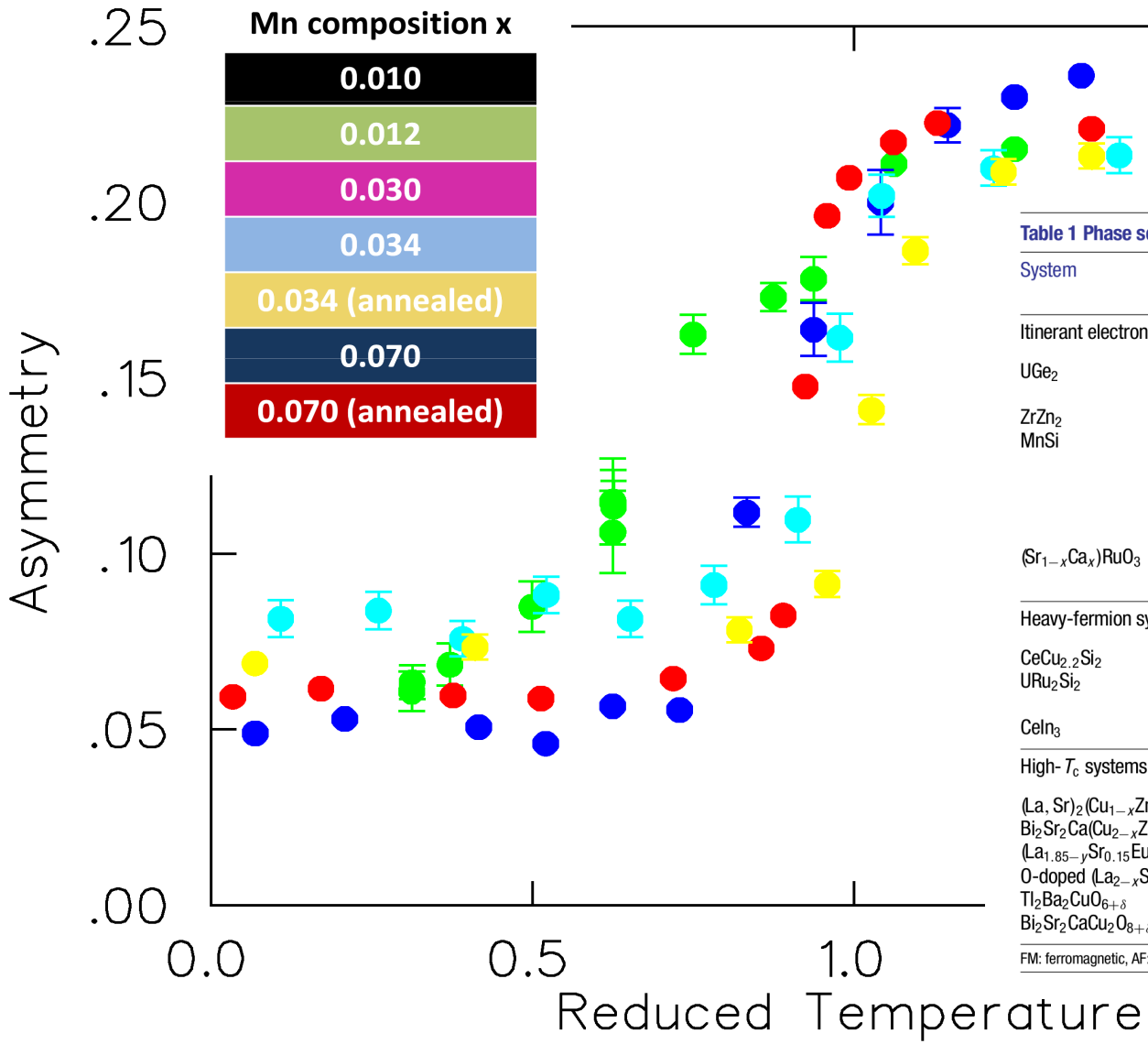

Table 1 Phase separation (PS)/first-order transition (FOT)/partial-volume (PVF) features detected

System	Crossover	Parameter (p in kbar)	FOT/PS/PVF
Itinerant electron magnets			
UGe_2	FM1–para	$p_c = 16$	FOT PS
$ZrZn_2$	FM–para	$p_c = 16.5$	FOT
MnSi	Helical–para	$12 = p^* < p < p_c = 14.6$	FOT
		$p < p_c$	FOT
		$p < 18$	PVF
		$p^* < p < p_c$	PS FOT
$(Sr_{1-x}Ca_x)RuO_3$	FM–para	$0.7 < Ca(x) < 0.65$	PS FOT
Heavy-fermion systems			
$CeCu_{2.2}Si_2$	AF(a)–SC	Temp.	PS
URu_2Si_2	AF–hidden	$3 < p < 10$	PVF
		$0 < p < 10$	PVF/FOT
$CeIn_3$	AF–SC	$p_c = 24.3$	FOT
High-T_c systems			
$(La, Sr)_2(Cu_{1-x}Zn_x)O_4$	SC–normal	$Zn(x)$	PS
$Bi_2Sr_2Ca(Cu_{2-x}Zn_x)O_8$	SC–fnormal	$Zn(x)$	PS
$(La_{1.85-y}Sr_{0.15}Eu_y)CuO_4$	Stripe–SC	$Eu(y)$	PS
O-doped $(La_{2-x}Sr_x)CuO_{4+y}$	Stripe–SC	Temp., $Sr(x)$	PVF/PS
$Tl_2Ba_2CuO_{6+\delta}$	SC–metal	Overdope $O(\delta)$	PS
$Bi_2Sr_2CaCu_2O_{8+\delta}$	SC–metal	Overdope $O(\delta)$	PS

FM: ferromagnetic, AF: antiferromagnetic, SC: superconducting phase, STM: Scanning tunnelling microscope.

S. R. Dunsiger et al, Nature Mater 9, 299 (2010)

Y. J. Uemura et al, Nature Physics 3, 29 (2007)

Summary

•**Fundamental Research :** µSR is invaluable in investigating magnetic ordering and excitations on a unique timescale largely inaccessible with other techniques. In addition, it is sensitive to spectral weight across the whole Brillouin zone. Often good timing resolution will be vital.

•**Device Applications** : as a local probe, µSR is particularly sensitive to heterogeneities, which place severe constraints on technological uses; it is well suited to dilute magnetic systems. Complementary depth resolved spin resonance techniques like LE-µSR provide unique opportunities to explore interlayer coupling and excitations in artificial heterostructures, of importance to understand spin decoherence.

Typical μSR spectra

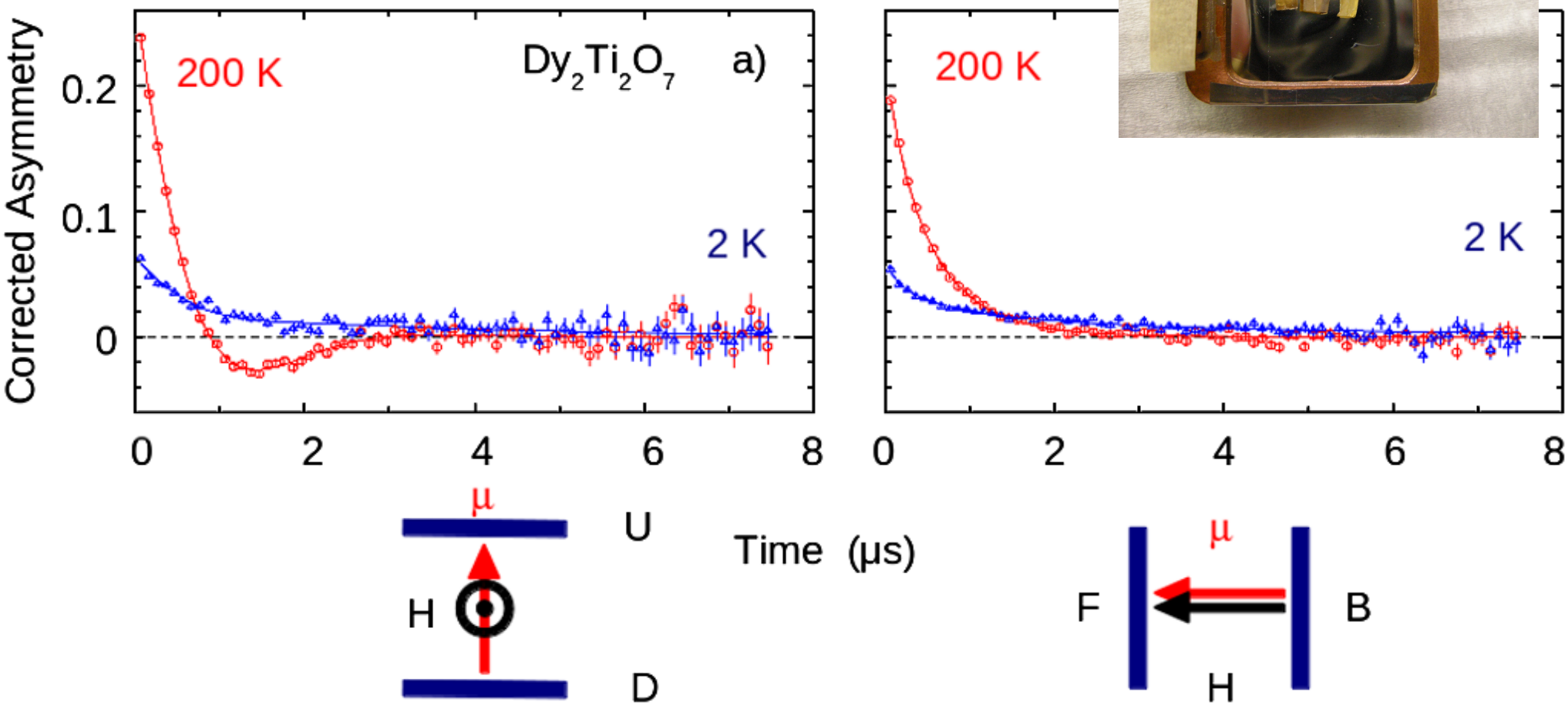

Earlier work on powder: J. Lago et al, J Phys Condens Matter 19, 1 (2007)

Synthesis of $Ga_{1-x}Mn_xAs$ Heterostructures using Nonequilibrium Molecular Beam Epitaxy Techniques

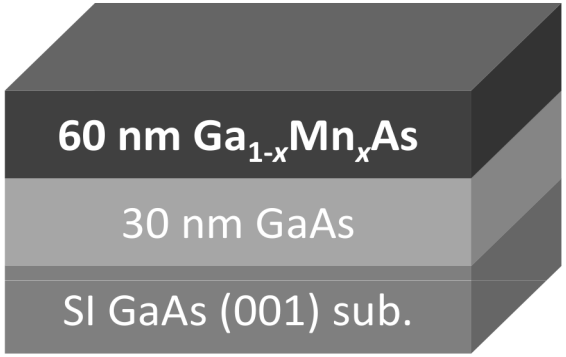

T_S ~ 230-250°C

T_S ~ 560°C

Growth rate: 12 nm/min

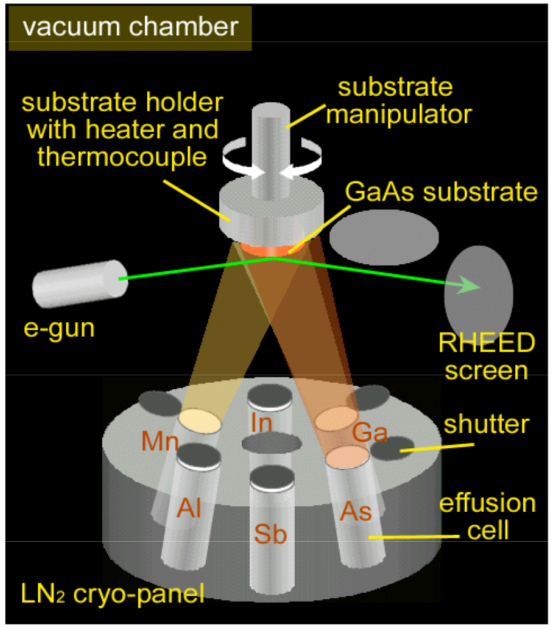

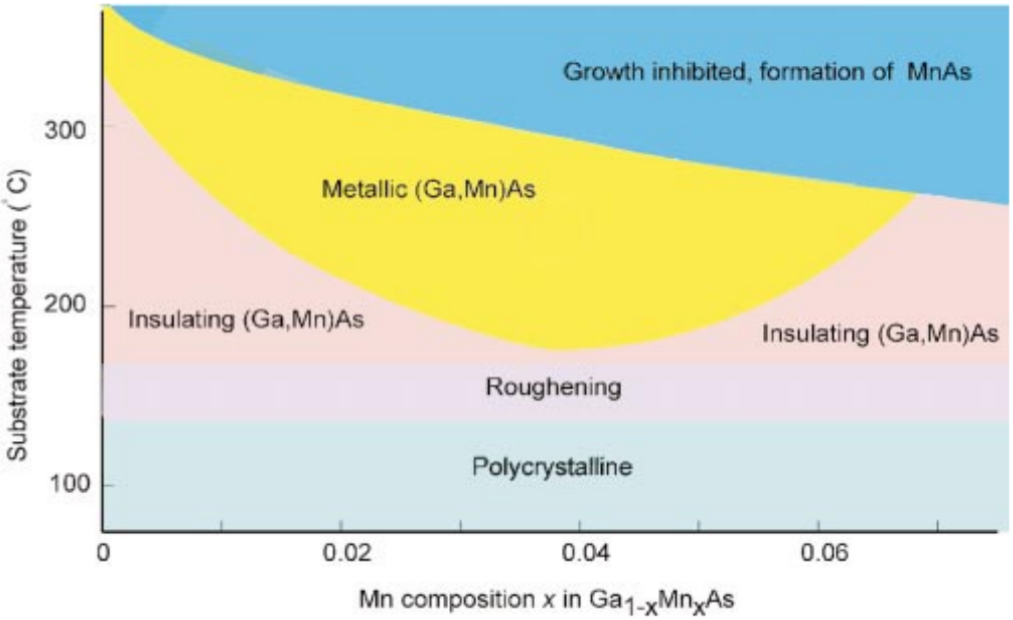

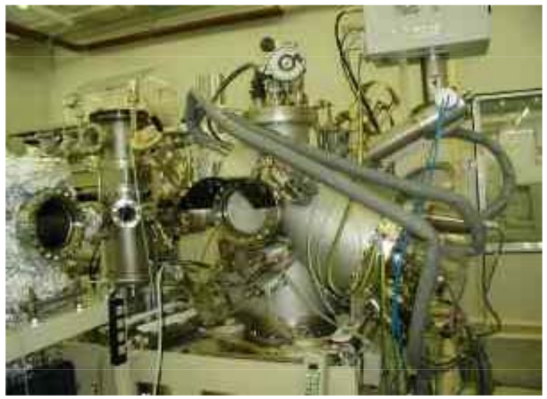

ULVAC MBC-1000 (Tohoku Univ.)

H. Ohno, Science 281, 951 (1998)

Schematic diagram of μSR Spectrometer : Anisotropic β Decay

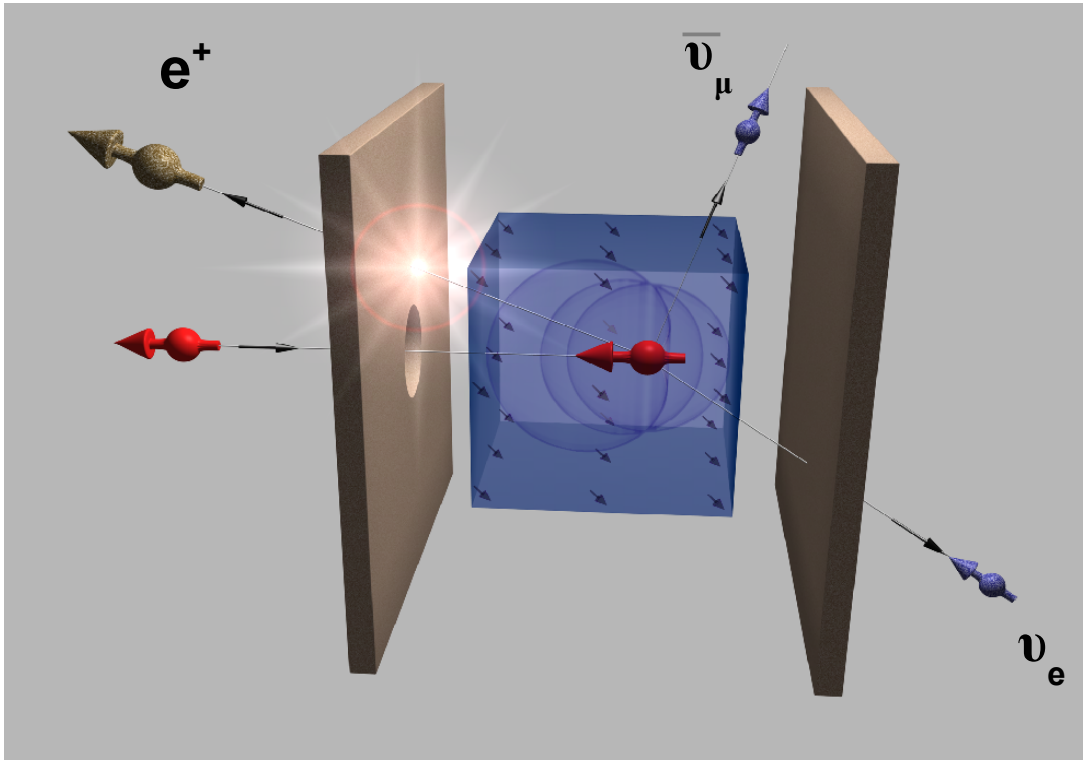

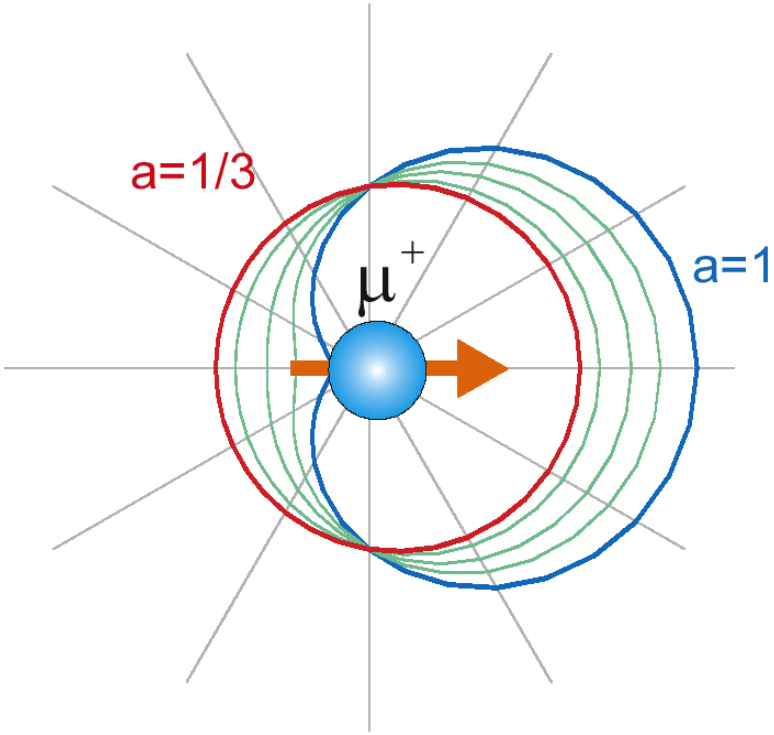

Probability of positron emission as a function of angle from the muon spin, at various positron energies; Lifetime=2.197 μs

Li(Zn,Mn)As as a new generation ferromagnet based on a I–II–V semiconductor

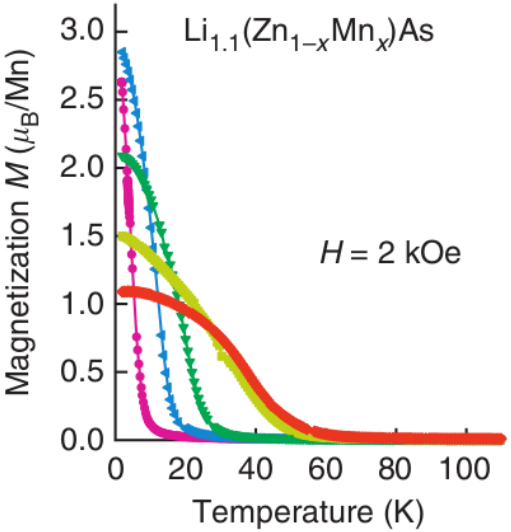

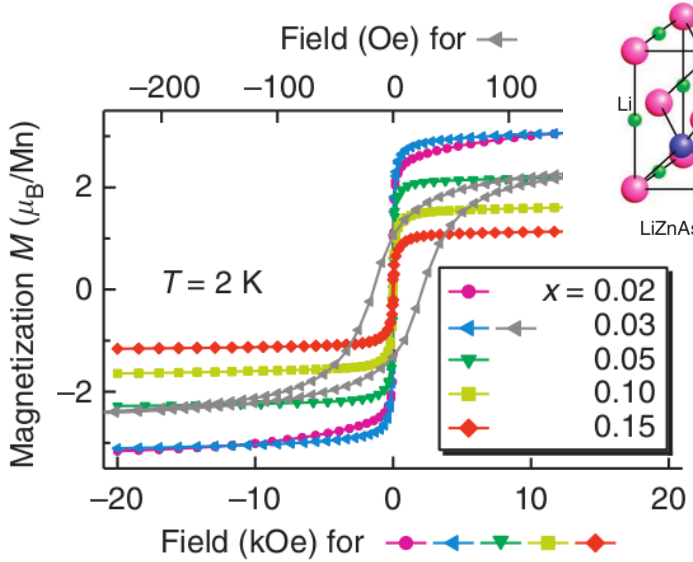

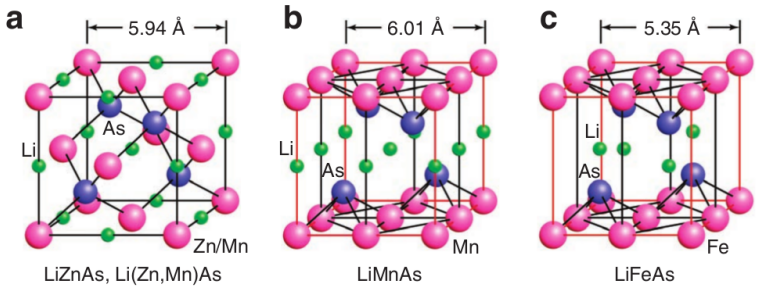

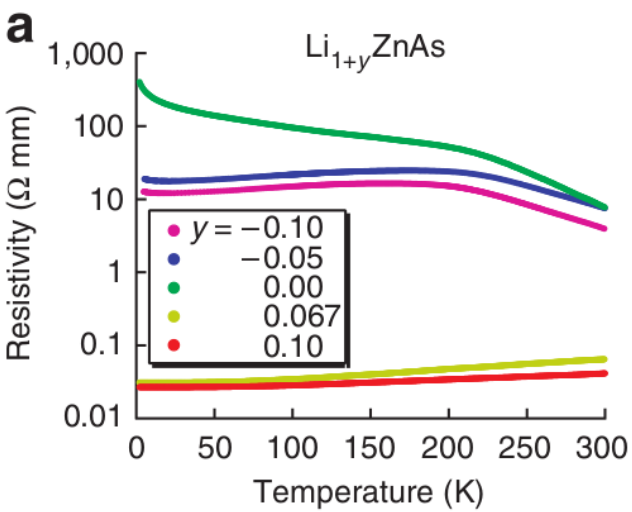

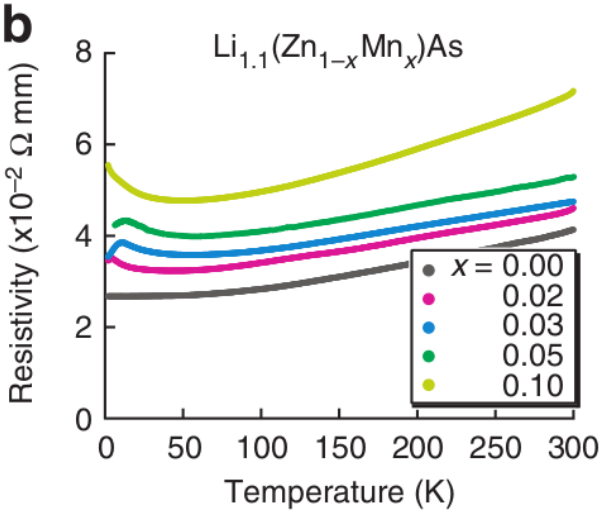

Z Deng et al, Nature Communications 2, 422 (2011)

Distinction of Heterogeneous Behaviour using μSR

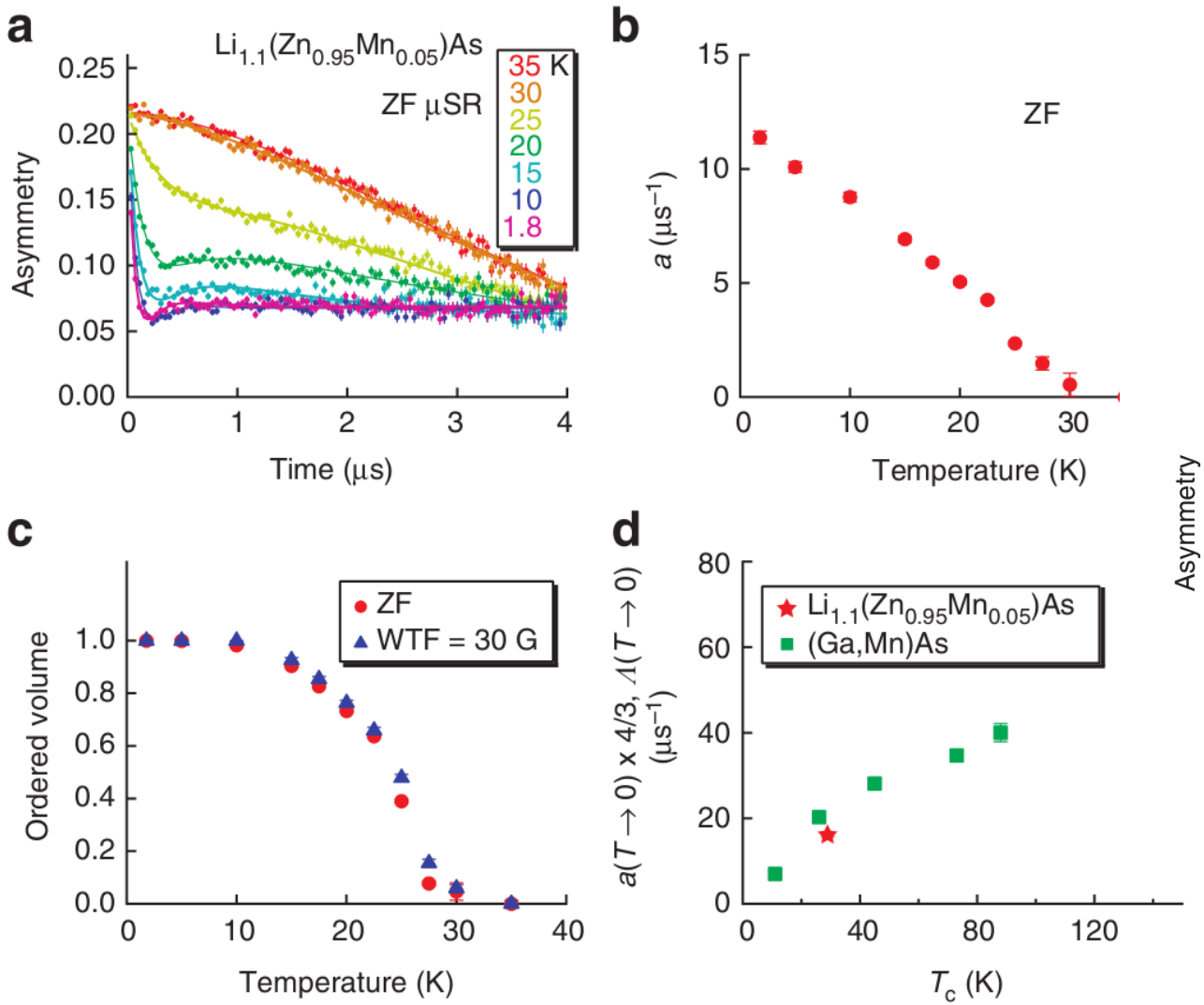

wTF : weak Transverse Field
ZF : Zero Field

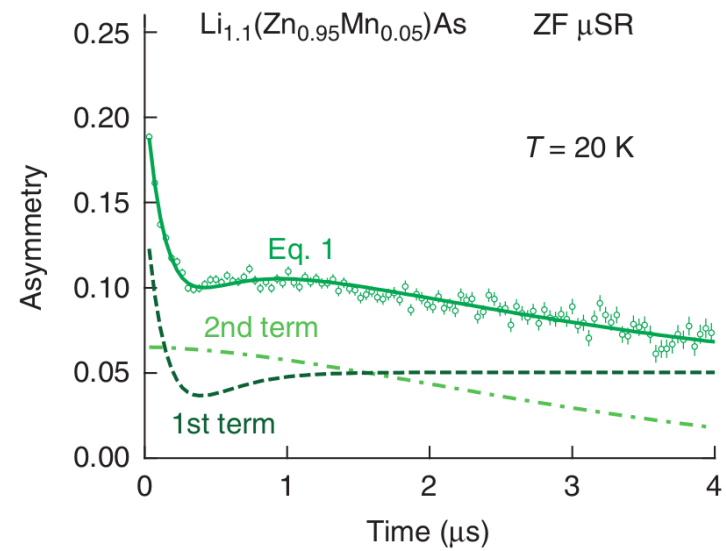

Z Deng et al, Nature Communications 2, 422 (2011)

LEλμSR – Local Probe of Internal Magnetic Field Distribution on nanometre Lengthscales

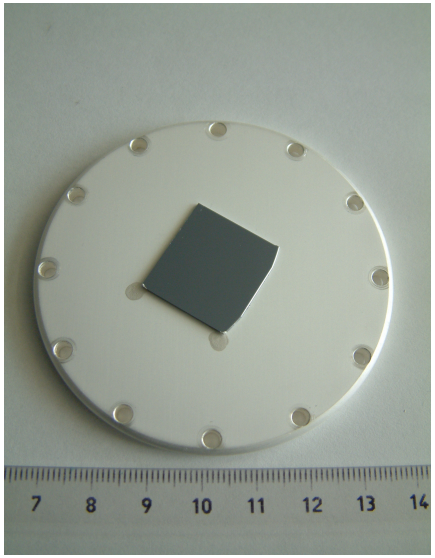

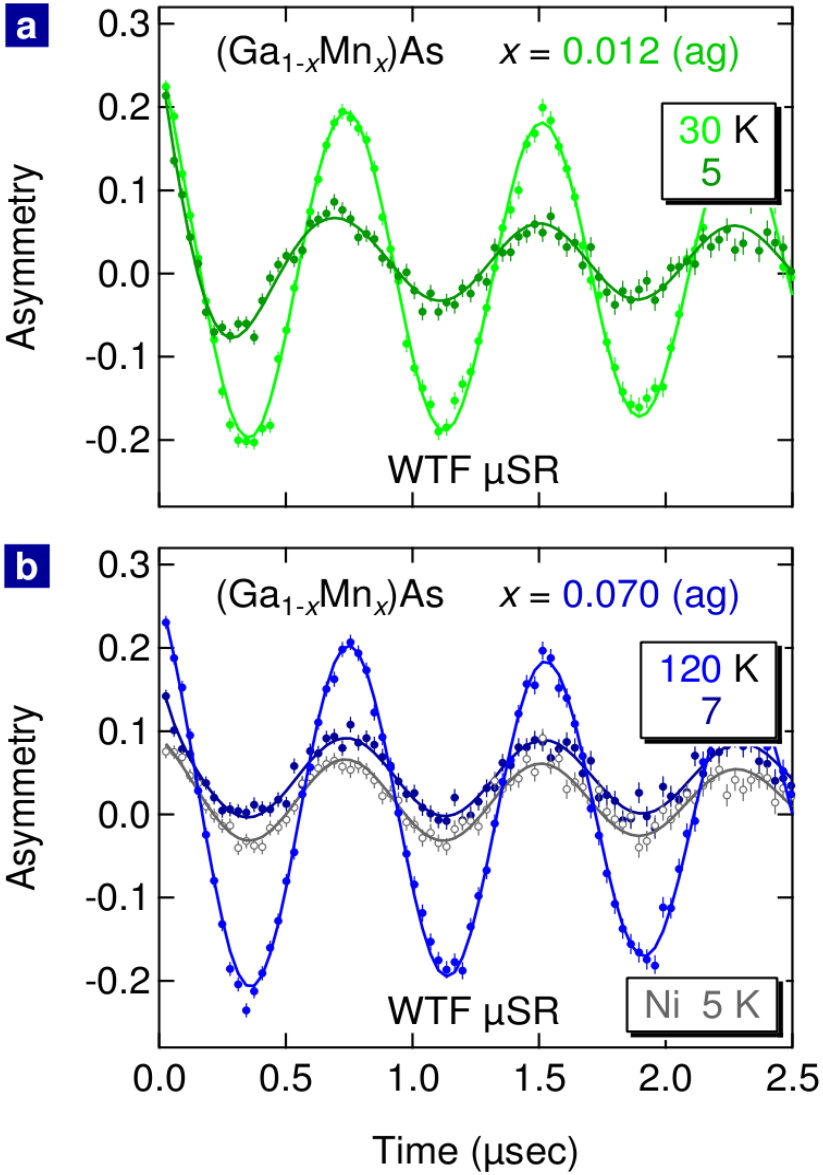

100 Oe // surface along [100]

Systematic homogeneous spin freezing involving the entire volume fraction observed on both sides of the semiconducting-metal transition

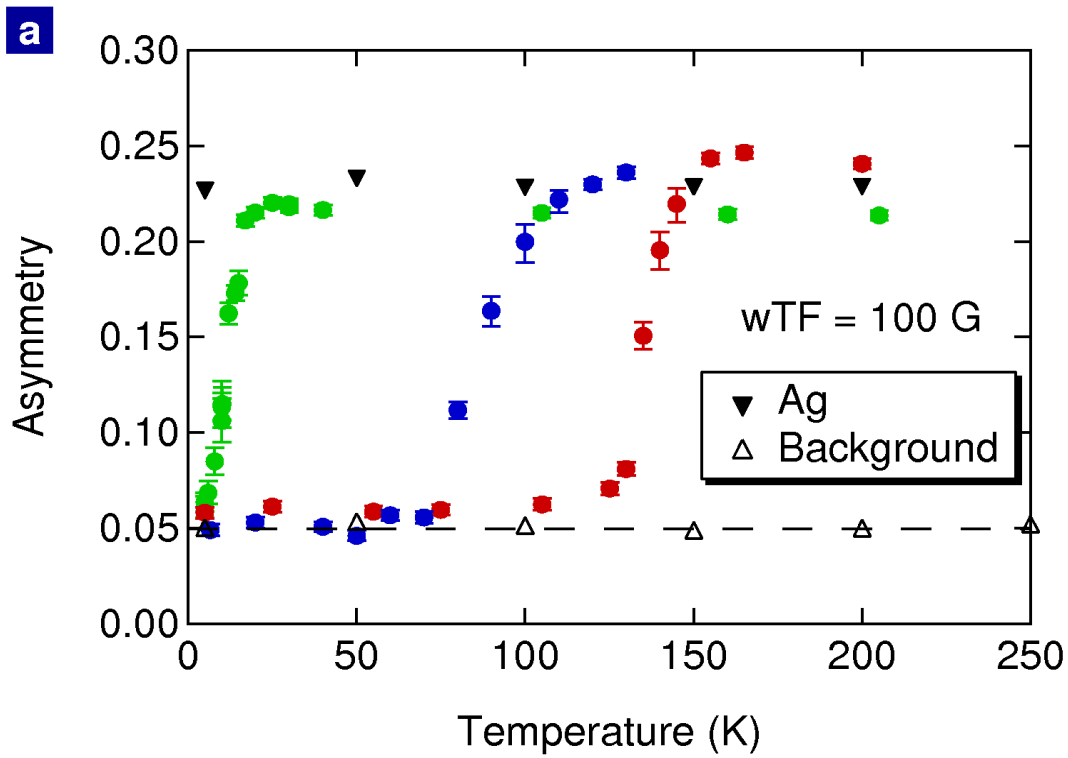

Mn composition x

- 0.010
- 0.012
- 0.030
- 0.034
- 0.034 (annealed)
- 0.070
- 0.070 (annealed)

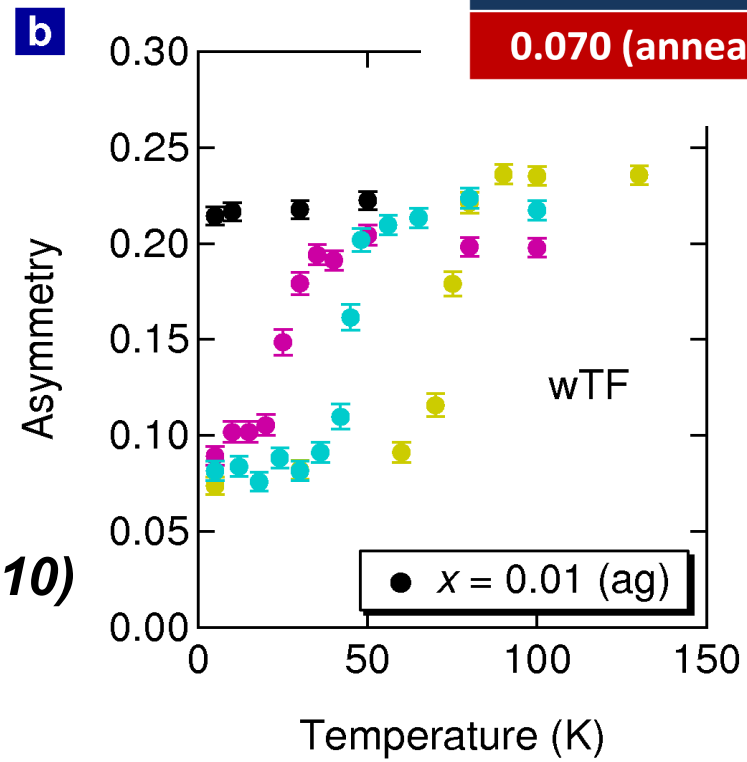

S. R. Dunsiger et al, Nature Mater 9, 299 (2010)

Red Shift of Optical Conductivity

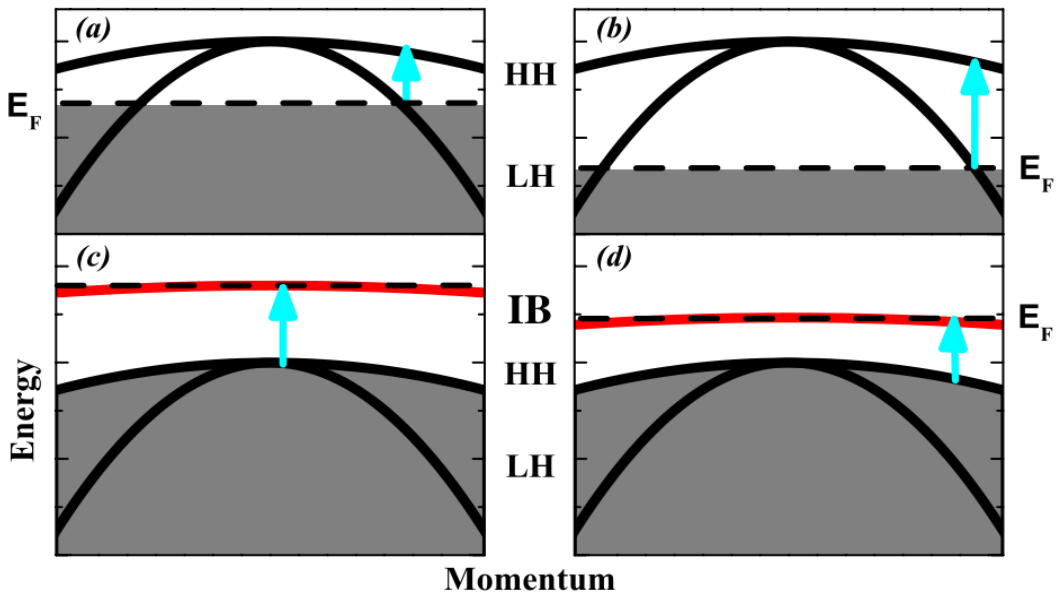

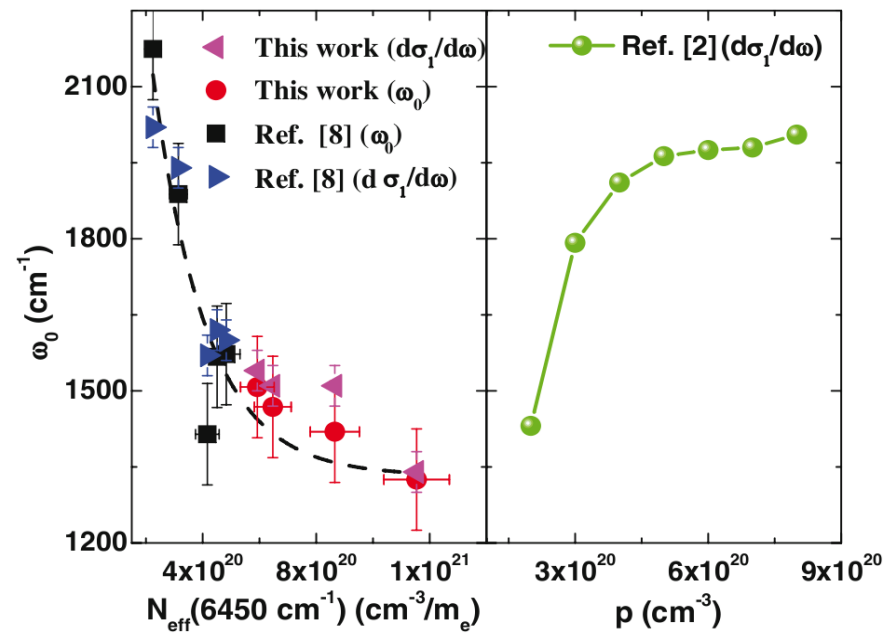

K. S. Burch et al, Phys Rev Lett 97, 087208 (2006)

Evolution of Magnetic Correlations with Chemical Potential

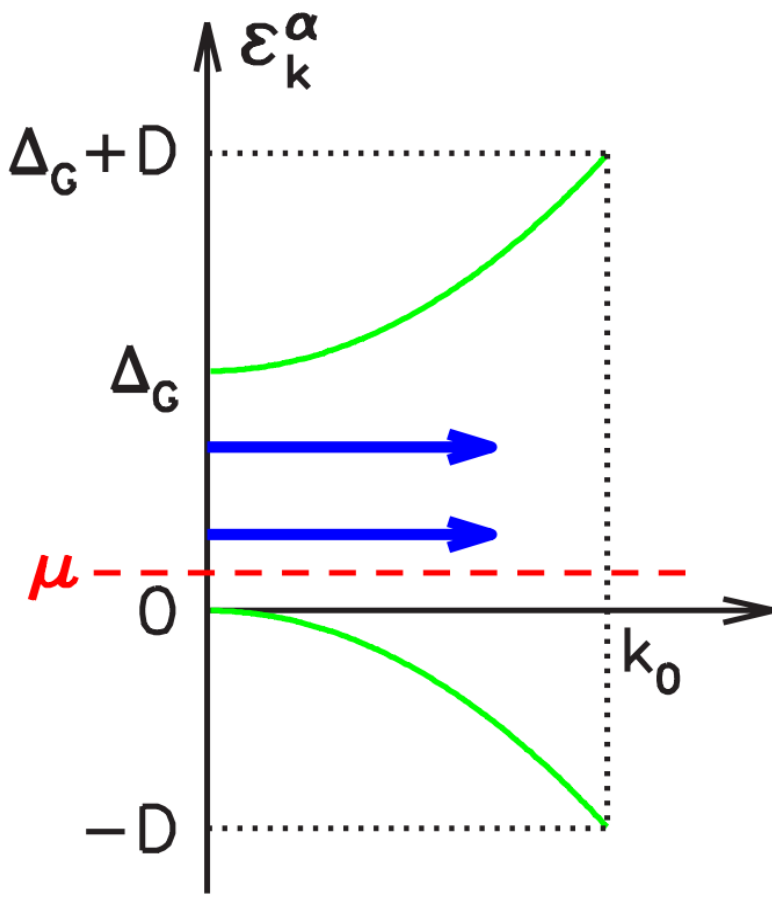

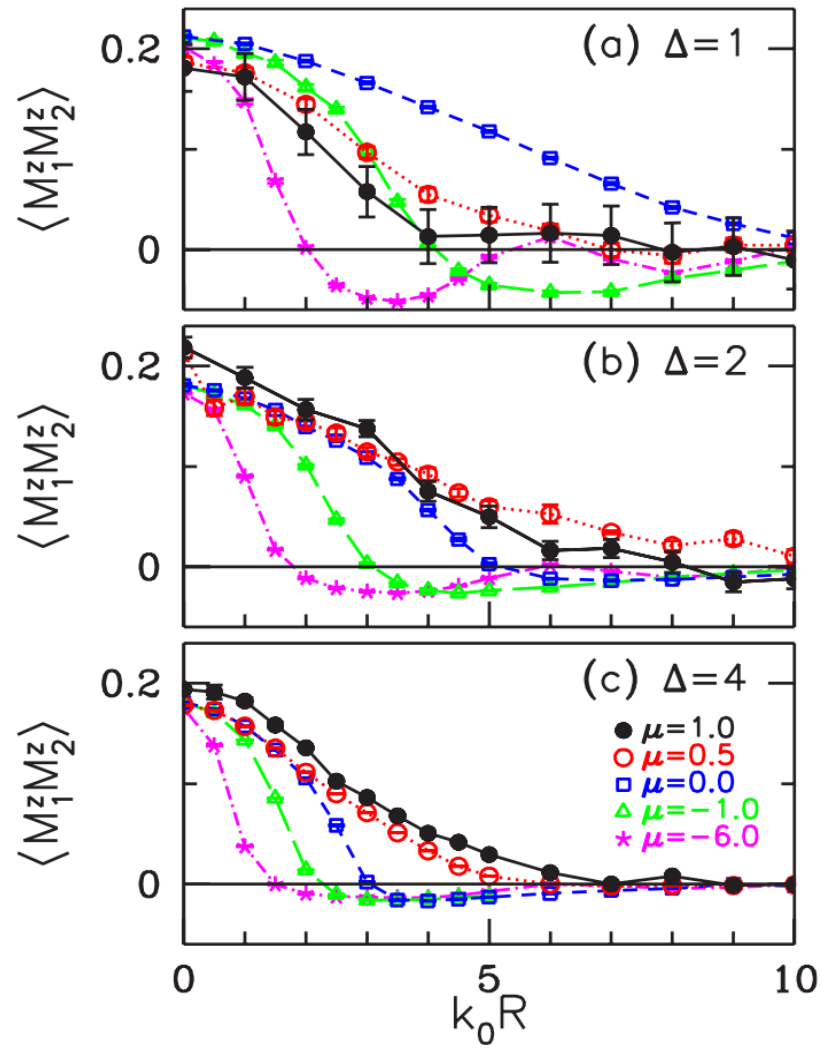

N. Bulut et al, Phys Rev B 76, 045220 (2007)